# Atomistic Insight on the Charging Energetics in Sub-nanometer Pore Supercacitors

**5 AUTHORS**, INCLUDING:

Jingsong Huang
Oak Ridge National Laboratory
**62** PUBLICATIONS   **1,792** CITATIONS

SEE PROFILE

Bobby Sumpter
Oak Ridge National Laboratory
**452** PUBLICATIONS   **7,684** CITATIONS

SEE PROFILE

Vincent Meunier
Rensselaer Polytechnic Institute
**238** PUBLICATIONS   **6,316** CITATIONS

SEE PROFILE

Guang Feng
Huazhong University of Science and Techn…
**47** PUBLICATIONS   **797** CITATIONS

SEE PROFILE

# Atomistic Insight on the Charging Energetics in Subnanometer Pore Supercapacitors

## Guang Feng,[†] Rui Qiao,*[,†] Jingsong Huang,[‡] Bobby G. Sumpter,[‡] and Vincent Meunier[§]

*College of Engineering and Science, Clemson University, Clemson, South Carolina 29634-0921, United States, Oak Ridge National Laboratory, Oak Ridge, Tennessee 37831-6367, United States, and Department of Physics, Applied Physics, and Astronomy, Rensselaer Polytechnic Institute, Troy, New York 12180-3590 United States*

Electrodes featuring subnanometer pores are favorable to the capacitance and energy density of supercapacitors. However, there is an energy penalty to enter subnanometer pores as ions have to shed part of their solvation shell. The magnitude of such an energy penalty plays a key role in determining the accessibility and charging/discharging of these subnanometer pores. Here, we report on the atomistic simulation of $Na^+$ and $Cl^-$ ions entering a polarizable slit pore with a center-to-center width of 0.82 nm. We show that the free energy penalty for these ions to enter the pore is less than 14 kJ/mol for both $Na^+$ and $Cl^-$ ions. The surprisingly small energy penalty is caused by the van der Waals attractions between ions and pore walls, the image charge effects, the moderate (19−26%) dehydration of the ions inside the pore, and the strengthened interactions between ions and their hydration water molecules in the subnanometer pore. The results provide strong impetus for further developing nanoporous electrodes featuring subnanometer pores.

## 1. Introduction

Supercapacitors are emerging as an ideal solution to electrical energy storage applications that require high power density and extraordinary cyclability.[1] However, the key factor limiting the widespread deployment of supercapacitors in everyday technology is their moderate energy density. Although energy density has long been limited to values well below 10 Wh/kg,[2] recently synthesized porous carbon electrodes with subnanometer pores exhibit an anomalous increase in normalized capacitance, thereby triggering great interest in using subnanometer pores for improving supercapacitors' energy density.[3] Such a breakthrough in the application of subnanometer pores challenges the long-held presumption that pores smaller than the size of solvated ions, on the order of 1 nm, do not contribute to energy storage. Fundamentally, the energy that ions have to acquire to shed part of their solvation shell in order to enter subnanometer pores is key to determining the pore accessibility, charging kinetics, and ultimately the energy and power density of supercapacitors based on these pores. A too large energy penalty would be detrimental for the capacitor charging performance, resulting in deteriorated power density. In contrast, a small energy penalty would be an important indication of the critical and urgent need for developing electrodes featuring subnanometer pores.

This outstanding problem is well suited for atomistic simulations. Prior molecular dynamics (MD) simulations indicate that the free energy penalty for a $Na^+$ ion entering a (10,10) carbon nanotube (CNT) with a center-to-center diameter of 1.34 nm is 3−6 kJ/mol but increases to 120 kJ/mol (or equivalently 1.24 eV in electrode voltage) in a (6,6) neutral CNT with a center-to-center diameter of 0.82 nm due to strong dehydration of ions.[4,5] Although these studies provide insights into the general behavior of ions in nanopores, the applicability of the results

for pores in supercapacitors remains unclear because these earlier studies focused on pores featuring nonpolarizable walls, whereas the pore walls in supercapacitors are clearly polarizable. Using the free energy penalty for a $Na^+$ ion to enter a neutral 0.82 nm wide CNT obtained in these studies to infer the voltage necessary to drive ions into the CNT suggests that, for the ions to enter the pore, a potential difference of 2.48 V must be applied between a supercapacitor's two electrodes (assuming a symmetric capacitor). This is in stark contradiction with existing experimental observations, where the capacitors featuring subnanometer pores often operate around 1 V with aqueous electrolytes.[3b] In this study, we use MD simulations to investigate the free energy penalty for small inorganic ions to enter 0.82 nm wide slit pores. To simulate real electrode behavior, herein, pore walls are modeled as ideally polarizable surfaces during the calculation of electrostatic interactions. We chose to study slit pores instead of cylindrical pores, in part, due to difficulties in the implementation of the present algorithm for enforcing a constant electrical potential on cylindrical pore walls. Additionally, some of the subnanometer pores in porous carbon electrodes are thought to have a slit shape.[3a,6] The present work is the first step along the line of charging energetics of ions entering polarizable pores, and the insights obtained here will be helpful for future studies using cylindrical pores. We show that, although the ions inside such pores lose 19−26% of their hydration shell, the energy penalty for these ions to enter the slit pore is less than 14 kJ/mol, which is only about 3−4% of their bulk hydration energies. This small energy penalty is rationalized by breaking it down into various contributions, including some terms considered for the first time in such systems.

## 2. Simulation Method and Models

As shown in Figure 1, the MD system considered here features a pair of pores connected to an electrolyte bath. The coordinate system is chosen such that $z = 0$ corresponds to the central plane of the two slit pores. Each slit pore is made of two graphene layers separated by a center-to-center distance of

* To whom correspondence should be addressed. E-mail: rqiao@clemson.edu.
† Clemson University.
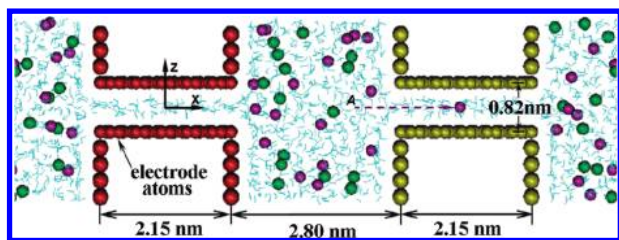‡ Oak Ridge National Laboratory.
§ Rensselaer Polytechnic Institute.

Subnanometer Pore Supercapacitors

*J. Phys. Chem. C, Vol. 114, No. 41, 2010* **18013**



**Figure 1.** Snapshot of the MD simulation system. Red and gold spheres denote the electrode atoms. Green and purple spheres denote Na$^+$ and Cl$^-$ ions, respectively. Cyan lines denote water molecules. Periodic boundary conditions were used in all three directions. Not all ions are shown for clarity.

0.82 nm, i.e., the same as those in earlier nanopore studies.[4,5] Because of the finite size of the carbon atoms, the actual ion-accessible width in the slit is about 0.48 nm. The length of both slit pores is chosen as 2.15 nm so that the hydration of an ion located at the middle portion of the pore is not affected by the ions and water molecules outside the pore. The width of the electrolyte bath, that is, the distance between the two slit pores along the pore axis direction, is taken as 2.8 nm so that a bulklike behavior for the electrolyte is obtained in its central portion. A 2.0 M NaCl solution is used as the electrolyte. Na$^+$ and Cl$^-$ ions are chosen because the sizes of ions used in typical aqueous electrolyte-based supercapacitors fall within the size of these ions. Because the ion-accessible width of the slit is smaller than the hydration diameter of Na$^+$ and Cl$^-$ ions (0.72 and 0.66 nm, respectively[7]), partial desolvation of ions is expected as the ions enter the pore. In computing the electrostatic interactions in the MD system, the polarizability of electrode atoms is explicitly addressed by enforcing the electric potential on the image plane of each electrode to a uniform and fixed value using the method developed in ref 8. Therefore, from an electrostatic interaction perspective, the electrode surface (or more precisely, its image plane) is a smooth and equal-potential surface, and thus, the polarizability of the electrode atoms is accounted for at the continuum level without introducing polarizability to individual electrode atoms. Independent simulations also show that such a method can predict the image charge force experienced by an ion near electrode surfaces accurately. Here, the image planes of the electrode surfaces are positioned at 0.08 nm from the geometrical planes of their atomic centers, in accordance to previous quantum mechanical calculations.[9] All carbon atoms are fixed in space during the simulation. The SPC/E model was used for the water molecules,[10] and Na$^+$/Cl$^-$ ions were modeled as charged Lennard-Jones (LJ) atoms with the LJ parameters for the Na$^+$ and Cl$^-$ taken from ref 11. The LJ parameters for the carbon atoms were taken from ref 12. Periodic boundary conditions were used in all three directions. The number of water molecules and ions were tuned so that, when the electric potentials on both electrodes are equal, the water and ion concentrations at the center of the electrolyte bath are equal to those of a bulk 2.0 M NaCl solution with $T = 300$ K and $P = 1$ bar.

Simulations were performed using a modified Gromacs package.[13] The temperature of the system was maintained at 300 K using a Berendsen thermostat. The particle mesh Ewald (PME) method complemented by the method developed in ref 8 was used to compute the electrostatic interactions.[14] An FFT grid spacing of 0.11 nm and cubic interpolation for charge distribution were used in the PME algorithm. A cutoff distance of 1.1 nm was used in the calculation of electrostatic interactions in the real space. The auxiliary Laplace equation required by the method in ref 8 is discretized using the compact fourth-
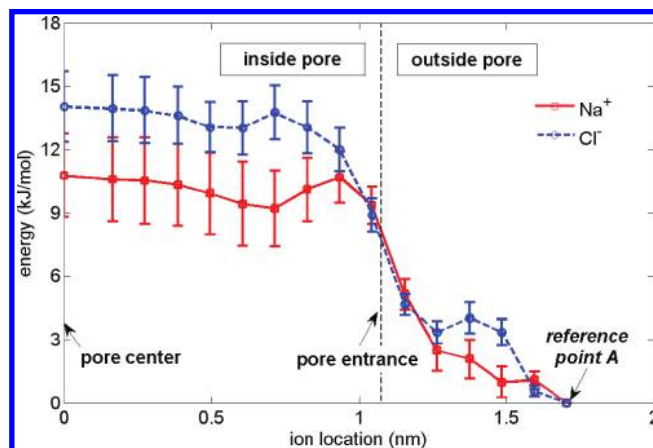


**Figure 2.** Potential of mean force (PMF) for Na$^+$ and Cl$^-$ ions located at the central plane of the pore, but different axial positions. The PMF at a position 0.63 nm away from the pore entrance into the electrolyte bath (point A in the figure) was taken as zero.

order stencil[15] on a uniform grid with a spacing of 0.11 nm. The Laplace equation is solved at each MD step. The nonelectrostatic interactions were computed by direct summation with a cutoff length of 1.1 nm. The bond length and angle of the water molecules were maintained using the LINCS algorithm.[16] To measure the potential of mean force (PMF) for an ion entering the electrode pores under zero potential polarization (i.e., the electric potential on each electrode is zero), the method in ref 5a was used. Specifically, ions were constrained on the central plane of the pores. The PMF at position $x$ along the pore central plane is obtained by

$$\text{PMF}(x) = -\int_{r_{ref}}^{x} f_x(x', y, z = 0)\,dx' \qquad (1)$$

where $f_x(x', y, z = 0)$ is the mean force along the slit direction experienced by an ion located on the central plane of the pore at position $x'$. $r_{ref}$ is a reference point in the bulk where the PMF is taken as zero. In this work, $r_{ref}$ is located at a position 0.63 nm from the pore entrance into the bulk electrolyte because the mean force experienced by ions located further into the electrolyte bath is very small. Using such an approach, we computed only the energy cost for an ion moving from the bulk electrolyte into the pore along the pore central plane, as indicated by the dashed arrow in Figure 1, and thus cannot explore the energy cost for an ion moving from the bulk electrolyte to a position off the central plane inside the pores. Such a limitation can be resolved by computing two-dimensional PMFs.[17] However, although computing two-dimensional PMFs is feasible in simulations involving nonpolarizable systems, it is computationally more expensive in the present systems where the polarizability of the pore surface is explicitly accounted for. Furthermore, because independent unconstrained simulations indeed show that the pore central plane is the most favorable position of ions inside these slits, the PMF computed here is sufficient to provide a basic understanding of the energy cost for an ion to enter polarizable subnanometer pores. To ensure statistical accuracy of the results, the mean force at each position is averaged from five independent simulations each lasting 2.5 ns.

## 3. Results and Discussion

Figure 2 shows the PMFs of Na$^+$ and Cl$^-$ ions along the pore axis. The PMF generally increases as the ions approach
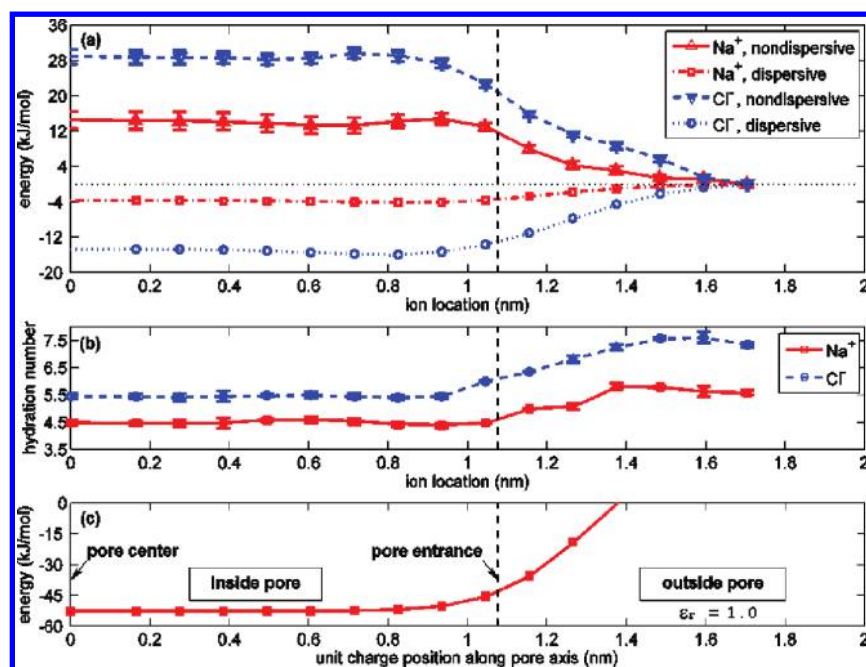
**Figure 3.** (a) Two components of the PMFs for $Na^+$ and $Cl^-$ ions, as defined in the text. (b) Hydration number of $Na^+$ and $Cl^-$ ions located at the central plane of the pore, but different axial positions. (c) Potential energy of a unit charge located at the central plane of the pore, but different axial positions due to image charge effects.

the pore center. To reach the pore center, the corresponding free energy penalties for $Na^+$ and $Cl^-$ ions are 10.8 ± 2.0 and 14.0 ± 1.7 kJ/mol, respectively. These values (<6 $k_BT$ or 0.15 eV) for the energy penalties are only 3–4% of the bulk hydration energy (see discussions below) and are much smaller than the high value of 120 kJ/mol reported for a $Na^+$ ion entering a 0.82 nm wide CNT electrode.[4] This is the key finding of this work, and it indicates that the $Na^+$ and $Cl^-$ ions can enter the pores readily when an electric potential difference of only ca. 300 mV is imposed between the two electrodes. We note that the energy penalty obtained here represents an upper limit of the energy penalty for ion entrance. This is due to several reasons. First, only one layer of atoms is modeled for each electrode wall in this study, but additional layers (which may occur in most materials) help lower the energy penalty through dispersive interactions (cf Figure 3a and the discussion below). Second, during the PMF calculation, no ion other than the probing ion were observed in the pore. In reality, there might be a small amount of ions inside the pore under zero polarization (this can be inferred from the energy cost of 4–6 $k_BT$ found here), and these ions can lower the barrier for other ions to enter the pore. Nevertheless, it is important to note that the energy penalty for ion entrance is already much smaller than that reported for nonpolarizable CNTs with the same size, and this supports the concept that subnanometer pores are accessible to ions even though partial ion desolvation is required. It is worth pointing out that experimental capacitive behavior in subnanometer pores typically does not show up in a galvanostatic charging until the potential difference is above ca. 200 mV (Figure S4A of ref 3a), indicating the presence of equivalent series resistances (ESRs). Contributions to the ESR of supercapacitors include electronic resistance of the electrode active materials, the contact resistance between the electrode and the current collector and between active material particles, the resistance of electrolyte that is associated with the mass transport, and the intrinsic resistance of the electrolyte.[18] We note that the desolvation energy penalty could also contribute to the Ohmic IR drop, but their relative importance compared

to the aforementioned mechanisms remains to be clarified experimentally.

To better understand these small PMF values, we decompose each PMF into two components: a dispersive component due to the dispersive ion–pore wall interactions (modeled using the LJ potential in our simulations) and a nondispersive component due to all other interactions. Figure 3a shows these two components for $Na^+$ and $Cl^-$ ions. We observe that the dispersive ion–pore wall interactions contribute to a significant reduction of the free energy penalty by 3.8 kJ/mol (14.8 kJ/mol) for a $Na^+$ ($Cl^-$) ion as it enters the pore. These results highlight the important role of the van der Waals forces in the adsorption of molecules in nanoconfined systems, which have also been shown to play a key role in the encapsulation of organic molecules inside CNTs,[19] and the desolvation of organic electrolyte ions and their subsequent contact adsorptions on uncharged electrode surfaces.[26] In contrast, in the absence of the dispersive ion–pore wall interactions, the free energy penalty for the $Na^+$ and $Cl^-$ ions to enter the pore is 14.5 and 28.8 kJ/mol, respectively. These energy penalties can be further decomposed into the partial dehydration effects of ions as they enter the pore and image charge effects.

First, as an ion enters the pore, it sheds part of its hydration shell due to confinement. This dehydration step is the main reason for the free energy penalty. Figure 3b shows the varying number of hydration water molecules (or hydration number) of the $Na^+$ and $Cl^-$ ions located at different positions along the pore axis. The water molecules belonging to the hydration shell of a given ion are defined as those within $r_1$ from the ion, where $r_1$ corresponds to the first local minimum of the ion–water pair correlation function. The hydration numbers of $Na^+$ and $Cl^-$ ions in the bulk electrolyte are close to those reported in earlier studies.[5] We observe that, as $Na^+$ and $Cl^-$ ions move from the bulk electrolyte to the pore center, their hydration number decreases by 19.3% and 25.8%, respectively. The free energy penalties for the ions entering the pore can be crudely estimated by the product of their hydration energy ($Na^+$, −375 kJ/mol; $Cl^-$, −347 kJ/mol[20]) with the relative reduction of their

Subnanometer Pore Supercapacitors

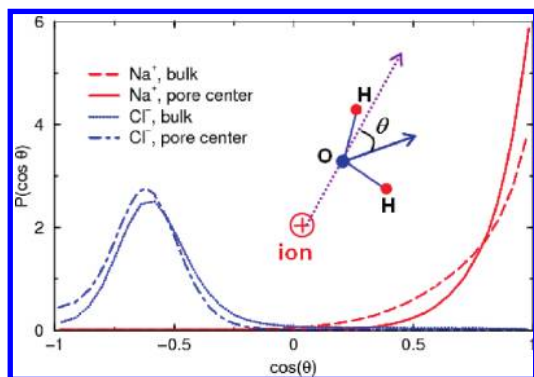*J. Phys. Chem. C, Vol. 114, No. 41, 2010* **18015**



**Figure 4.** Orientation distribution of the ion's hydration water molecules with respect to the ions located in the bulk electrolyte and in the pore center. A random distribution of the dipole of water with respect to the ion corresponds to a probability density of 0.5.

hydration number as they move from the bulk into the center of the pores, giving an energy penalty of 72.4 and 89.5 kJ/mol for the Na$^+$ and Cl$^-$ ions, respectively. These values are considerably larger than the energy of 14.5 and 28.8 kJ/mol shown in Figure 3a. The apparently lower free energy penalties are caused by the image charge effects (discussed below) and the facts that (1) the energetic cost to remove the first water in the hydration shell of an ion is less than that to remove the last water[5b] due to the balance of ion−water and water−water interactions and (2) the energetic cost of losing hydration water molecules as an ion moves from the bulk electrolyte to the pore center is partially compensated by the strengthened interactions between the ion and its remaining hydration water molecules. In fact, the interaction energy between a Na$^+$ (Cl$^-$) ion and each of its hydration water molecules increases by 9.8% (15%) from −82.3 (−40.8) to −90.4 kJ/mol (−46.9 kJ/mol) as it moves from the bulk electrolyte into the center of the slit pore. The fact that the interaction between an ion and its hydration water molecules increases inside the pores is not surprising: inside the pores, the dipole of each of its hydration water molecules is better aligned with the ion−water vector because its orientation is perturbed by fewer neighboring molecules. This is illustrated in Figure 4, which shows the orientations of the hydration water molecules of Na$^+$ and Cl$^-$ ions with respect to these ions located in the bulk electrolyte and in the pore center (cf. Figure 2). The orientation is quantified by the angle $\theta$ formed between the dipole of a hydration water molecule and the vector pointing from the ion to the oxygen atom of the water molecule (see the inset).

Second, an ion near or inside the pore is influenced by the polarizable media via an electrostatic interaction that can be treated using the concept of image charges. This interaction reduces the free energy of the system. We computed the variation of the potential energy of a unit charge along the pore axis due to such effects. Because water simultaneously serves as a hydration and dielectric medium for the ions and its dielectric constant $\varepsilon_r$ in the present system is unknown, we performed the calculations in vacuum by neglecting the water molecules and ions. Specifically, we removed all water molecules and ions from the system and placed a single ion along the pore axis. The potential energy at a position 0.3 nm away from the pore entrance was chosen as the zero value because, in real systems, the dielectric constant of water beyond this position approaches that of bulk electrolyte solution, and thus, the image charge forces weaken. The results shown in Figure 3c indicate that, in vacuum, an ion's free energy decreases by ∼53 kJ/mol as the ion enters the pore. Assuming that $\varepsilon_r$ has a

value of 5−20, as typically reported for water within a few angstroms from electrode surfaces,[21–24] the free energy gain is still ca. 3−11 kJ/mol. Thus, the presence of image charge clearly contributes to the reduction of the energy penalty.

## 4. Conclusion

The energy cost for small inorganic ions to enter ideally polarizable subnanometer pores is studied using MD simulations. Our simulations suggest that Na$^+$ and Cl$^-$ ions entering a 0.82 nm wide slit pore must overcome a free energy penalty of less than 14 kJ/mol. This small energy penalty is caused by the van der Waals attractions between each ion and the pore walls, image charge effects, the moderate (19−26%) dehydration of the ions inside the pore, and the enhanced interactions between ions and their hydration water molecules in the subnanometer pore. The energy penalty identified here is much smaller than that in 0.82 nm wide CNT pores (∼120 kJ/mol).[4] The difference is due to the much weaker energy associated with ion dehydration in our slit pores and the image force effects. More recent simulations[5b] showed that the energy penalty for a Na$^+$ ion to enter a 0.94 nm (center-to-center diameter) wide CNT, during which it loses a similar amount of hydration water as in the present slit pores, is ∼23 kJ/mol. This is in better agreement with our value for slit pores, with the main difference likely due to pore shape and to the fact that the image charge effects were absent in those simulations. The small energy penalty indicates that the Na$^+$ and Cl$^-$ ions can enter the pores readily. Such an energy penalty of 14 kJ/mol may translate to an electric potential difference of ca. 300 mV between the two pore electrodes, which may contribute partially to the IR drop at the initial stage on the experimental galvanostatic charging, although the precise contribution remains to be elucidated due to the complicated nature of the initial Ohmic IR drop. A recent reverse Monte Carlo simulation of center-to-center 1.2 nm wide slit-shaped pores with tetraethylammonium-tetrafluoroborate (TEA-BF$_4$) in propylene carbonate shows that the unpolarized pores are packed with electrolyte ions (Figure 3 in ref 25). We note that the pores in that work are larger and additionally that organic ions tend to have stronger dispersive interactions with the pore walls.[26] These and our results show that the energy cost for ions to enter pores inside supercapacitors is sensitive to the pore size, pore shape, and the nature of the electrolyte ions. Theoretical work comparing organic with aqueous electrolytes and comparing slit pores with cylindrical pores and experimental studies with the aid of the atomistic insight obtained in the present work should be pursued in order to further clarify the energy penalty experienced by various ions entering subnanometer pores.

### References and Notes

(1) (a) Conway, B. E. *Electrochemical Supercapacitors: Scientific Fundamentals and Technological Applications*; Kluwer Academic/Plenum: New York, 1999. (b) Miller, J. R.; Simon, P. *Science* **2008**, *321*, 651–652.

**18016** *J. Phys. Chem. C, Vol. 114, No. 41, 2010*

Feng et al.

(2) (a) Simon, P.; Gogotsi, Y. *Nat. Mater.* **2008**, *7*, 845–854. (b) Zhang, L. L.; Zhao, X. S. *Chem. Soc. Rev.* **2009**, *38*, 2520–2531.

(3) (a) Chmiola, J.; Yushin, G.; Gogotsi, Y.; Portet, C.; Simon, P.; Taberna, P. L. *Science* **2006**, *313*, 1760–1763. (b) Raymundo-Piñero, E.; Kierzek, K.; Machnikowski, J.; Béguin, F. *Carbon* **2006**, *44*, 2498–2507.

(4) Peter, C.; Hummer, G. *Biophys. J.* **2005**, *89*, 2222–2234.

(5) (a) Park, J. H.; Sinnott, S. B.; Aluru, N. R. *Nanotechnology* **2006**, *17*, 895–900. (b) Song, C.; Corry, B. *J. Phys. Chem. B* **2009**, *113*, 7642–7649.

(6) Shiratori, N.; Lee, K. J.; Miyawaki, J.; Hong, S.-H.; Mochida, I.; An, B.; Yokogawa, K.; Jang, J.; Yoon, S.-H. *Langmuir* **2009**, *25*, 7631–7637.

(7) Israelachvili, J. *Intermolecular and Surface Forces*; Academic Press: New York, 1992.

(8) Raghunathan, A. V.; Aluru, N. R. *Phys. Rev. E* **2007**, *76*, 011202.

(9) Lang, N. D.; Kohn, W. *Phys. Rev. B* **1971**, *3*, 1215–1223.

(10) Berendsen, H.; Grigera, J.; Straatsma, T. *J. Phys. Chem.* **1987**, *91*, 6269.

(11) Smith, D. E.; Dang, L. X. *J. Chem. Phys.* **1994**, *100*, 3757–3766.

(12) Cornell, W. D.; Cieplak, P.; Bayly, C. I.; Gould, I. R.; Merz, K. M., Jr.; Ferguson, D. M.; Spellmeyer, D. C.; Fox, T.; Caldwell, J. W.; Kollman, P. A. *J. Am. Chem. Soc.* **1995**, *117*, 5179–5197.

(13) Lindahl, E.; Hess, B.; van der Spoel, D. *J. Mol. Model.* **2001**, *7*, 306–317.

(14) Darden, T.; York, D.; Pedersen, L. *J. Chem. Phys.* **1993**, *98*, 10089–10092.

(15) Li, Z.; Ito, K. *The Immersed Interface Method: Numerical Solutions of PDEs Involving Interfaces and Irregular Domains (Frontiers in Applied Mathematics)*; Society for Industrial and Applied Mathematics: Philadelphia, 2006.

(16) Hess, B.; Bekker, H.; Berendsen, H.; Fraaije, J. *J. Comput. Chem.* **1997**, *18*, 1463.

(17) Allen, T. W.; Andersen, O. S.; Roux, B. *Biophys. Chem.* **2006**, *124*, 251–267.

(18) Pandolfo, A. G.; Hollenkamp, A. F. *J. Power Sources* **2006**, *157*, 11.

(19) Meunier, V.; Kalinin, S. V.; Sumpter, B. G. *Phys. Rev. Lett.* **2007**, *98*, 056401.

(20) Marcus, Y. *Ion Properties*; Marcel Dekker: New York, 1997.

(21) Conway, B. E.; Bockris, J. O'M.; Ammar, I. A. *Trans. Faraday Soc.* **1951**, *47*, 756.

(22) MacDonald, J. R.; Barlow, C. A., Jr. *J. Chem. Phys.* **1962**, *36*, 3062.

(23) Dzubiella, J.; Hansen, J.-P. *J. Chem. Phys.* **2005**, *122*, 234706.

(24) Huang, J.; Sumpter, B. G.; Meunier, V. *Chem.—Eur. J.* **2008**, *14*, 6614–6626.

(25) Tanaka, A.; Liyama, T.; Ohba, T.; Ozeki, S.; Urita, K.; Fujimori, T.; Kanoh, H.; Kaneko, K. *J. Am. Chem. Soc.* **2010**, *132*, 2112–2113.

(26) Feng, G.; Huang, J.; Sumpter, B. G.; Meunier, V.; Qiao, R. *Phys. Chem. Chem. Phys.* **2010**, *12*, 5468–5469.